

Performance of the most recent avalanche photodiodes for future X-ray and gamma-ray astronomy

J.Kataoka, T.Ikagawa, Y.Yatsu, Y.Kuramoto, T.Saito, N.Kawai,
Y.Serino, J.Kotoku, Y.Ishikawa, and N.Kawabata^b

^aTokyo Institute of Technology, Meguro, Tokyo, Japan

^bHamamatsu Photonics K.K., Hamamatsu, Shizuoka, Japan

ABSTRACT

We report on the performance of the most recent avalanche photodiodes produced by Hamamatsu Photonics, as low-energy X-rays and γ -rays detectors. APDs share good features of both photo diodes and PMTs, as they are very compact, produce an internal gain of 10–100, and have high quantum efficiency close to 100 % in the visible light. Until very recently, however, APDs were limited to very small surfaces, and were mainly used as a digital device for light communication. We have developed large area (up to 10×10 mm²) APDs which can be used in the physics experiments. The best energy resolution of 6.4 % (FWHM) was obtained in direct detection of 5.9 keV X-rays. The FWHM results of 9.4 % and 4.9 % were obtained for 59.5 keV and 662 keV γ -rays respectively, as measured with the CsI(Tl) crystal. The minimum detectable energy for the scintillation light was as low as 1 keV at lightly cooled environment (-20°C). Note that our results are the best records ever achieved with APDs. Various applications of APDs are presented for future space research and nuclear medicine. In particular 2-dimensional APD arrays will be a promising device for a wide-band X-ray and γ -ray imaging detector.

Keywords: avalanche photodiode, soft X-ray detector, scintillation γ -ray detector, nuclear imaging

1. INTRODUCTION

Photo diodes (PDs) have an excellent quantum efficiency (close to 100%) in the visible and near infrared. PDs work very stably with low bias voltage and provide compact and rugged structures. A drawback is that, they have no internal gain and in most cases require use of an amplifier to obtain a large enough signal. In such a low-signal applications, photomultiplier tube (PMT) is generally used because internal gain is very high and sufficient signal-to-noise ratio is available. Several disadvantages of using PMTs are that it is sensitive to magnetic field, has relatively low quantum efficiency for input light signal (20–30 %), and power consumption is rather high.

In recent years avalanche photodiodes (APD) have attracted considerable attention since good features of both PDs and PMTs are shared by APDs.²¹ In fact, APDs have the quantum efficiency close to 100% in the visible and near infrared, can be very compact and less affected by magnetic field, and produces an internal gain of 10–100 or more, though it is much less than typical PMT gain. Thus the basic properties of APD is well suited to read out small numbers of photons, so long as it has large detection area and is operated under stable conditions.

For a long time, however, APDs were limited to very small surfaces, and mainly used as a digital device for light communications (e.g., a receiver for optical fibers). During the past decade, a large area APDs operating as a linear detector has also been available. As a scintillation photon detector, Moszyński et al. (1998; 2001; 2003) have obtained a better or comparable energy resolution to those observed with a PMT. Moreover, operations of APDs at low temperature reduce the dark current noise contribution. This significantly improves the sensitivity to low-intensity signals, such as weak scintillation light produced by low energy X-rays.

In this paper, we report the performance of large area APDs recently developed by Hamamatsu Photonics K.K to determine its suitability as a low energy X-rays and γ -rays scintillation detector. After recalling APD structures, we summarize fundamental properties of three different APDs in §2. In §3, we present the performance

Further author information: (Send correspondence to J.K.)

J.K.: E-mail: kataoka@hp.phys.titech.ac.jp, Telephone: 81 3 5734 2388

of reach-through APD in direct detection of soft X-ray photons. In §4, we show the energy spectra of γ -ray sources measured with four different scintillators coupled to the reverse-type APDs. Various applications of APDs will be presented in §5. We particularly introduce future Japanese X-ray astronomy mission *NeXT*, a compact Anger camera and 32 ch APD array for nuclear medicine and physics experiments. Finally we summarize our results in §6.

2. APD STRUCTURES AND BASIC PARAMETERS

2.1. APD types

Three types of APDs have been developed by different manufactures: (a) “beveled-edge”, (b) “reach-through”, and (c) “reverse-type” diode. Structure (a), the “beveled-edge” diode is a traditional p⁺n junction in which the n-type resistivity is chosen so as to make the breakdown voltage very high (typically 2000 V). APDs developed by Advanced Photonix Inc (hereafter API) belongs to this type and most extensively studied in literature.^{11–14, 16, 17, 19} As a scintillation photon detector, the best result of 4.8 ± 0.14 % (FWHM) was obtained for 662 keV γ -rays using CsI(Tl) crystal coupled to 16 mm ϕ APD. Moreover, thanks to its wide depletion layer of ≥ 50 μm depth, this type of APD can also be used in direct detection of soft X-rays in the device.^{13, 15–17} An energy resolution of 9.3% (FWHM) was obtained for 5.9 keV X-rays.

Table 1. Parameters for Hamamatsu APDs tested in this paper.

| Name | SPL 2407 | S8664-55 | S8664-1010 |
|---------------------------|---------------|------------------------------|--------------------------------|
| Type | reach-through | reverse | reverse |
| Surface area | 3 mm ϕ | 5 \times 5 mm ² | 10 \times 10 mm ² |
| Dark current (G=30, 20°C) | 4.4 nA | 0.4 nA | 1.7 nA |
| Capacitance (G=30, 20°C) | 10.2 pF | 88 pF | 269 pF |
| Break-down voltage (25°C) | 647 V | 390 V | 433 V |

Structure (b), “reach through” type, applies to a diode in which the depletion layer comprises both a relatively wide drift region of fairly low field (~ 2 V/ μm) and a relatively narrow region of field sufficient for impact ionization (25–30 V/ μm). The advantage of such a structure is that only relatively low voltages (typically less than 500 V) are required to full depleting the devices. For example, SPL 2625 developed by Hamamatsu has a depletion layer of 130 μm thickness, and operates below 500 V.^{5, 6} Traditional reach-through APDs have a wide low-field drift region at the front of the device, with the multiplying region at the back. A disadvantage of this structure is that most of the dark current undergoes electron multiplication, resulting that large area devices tend to be somewhat noisy.

The “reverse type (c)” is specifically designed to couple with scintillators. This type is quite similar to the reach-through APD, but the narrow high-field multiplying region has been moved to the front end, typically about 5 μm from the surface of the device.^{8, 9} Since most scintillators emit at wavelength of 500 nm or less, most of lights from scintillators are absorbed within the first 1–3 μm of the depletion layer and generates electrons which undergo full multiplication. Whereas most of the dark current undergoes only hole multiplication, reducing the noise contribution significantly. Ikagawa et al. (2003) have tested reverse-type APD produced by Hamamatsu (S8664-55; see also below). Thanks to its low leakage current, this type of APDs records the best results for the detection of low energy X-rays and γ -rays.

In this paper, we summarize the basic properties of APDs most recently developed by Hamamatsu (see Table 1): SPL2407, S8664-55, and S8664-1010N. SPL2407 is a reach-through type, whereas S8664-55 and S8664-1010N are the reverse-type APDs. SPL 2407 (3mm ϕ) has a depletion layer of 130 μm thickness, and can be used in direct detection of soft X-rays below 15 keV. S8664-1010N (10 \times 10 mm²) is a prototype APD developed on the technical base of S8664-55 (5 \times 5 mm²), except that the dead layer of S8664-1010N is thinner than that of S8664-55. With a short review of Ikagawa et al. (2003; 2004), we will study reverse-type APDs for scintillation detection from 5.9 keV to 662 keV.

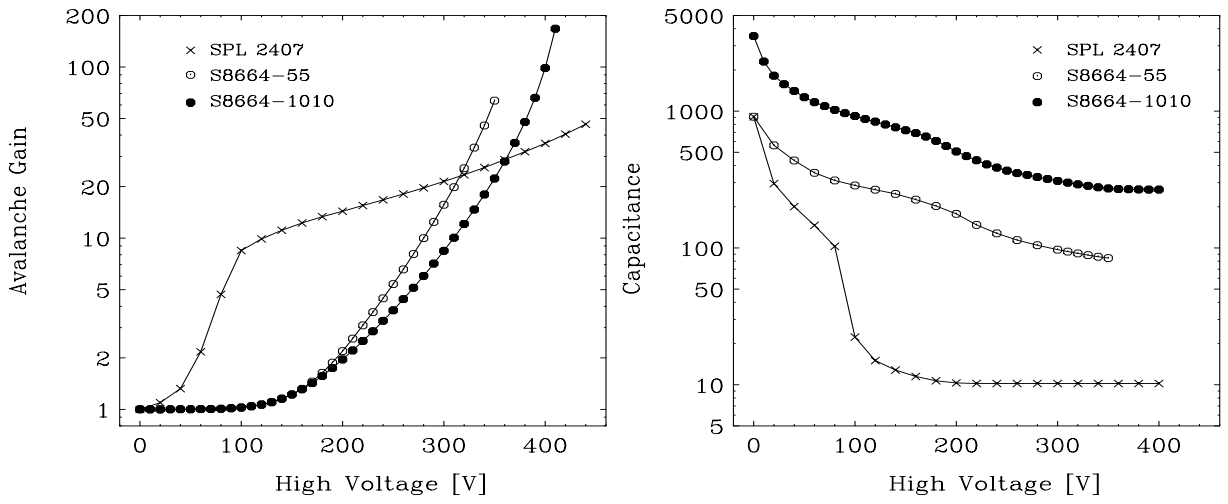


Figure 1. Gain (*left*) and capacitance (*right*) variations of Hamamatsu APDs measured at room temperature ($+20^{\circ}\text{C}$).

2.2. Gain and capacitance

The gain characteristic of APDs can be measured under constant illumination of monochromatic light source recording the photocurrent of the APD as a function of bias voltage. We use a light emitting diode (LED) producing light signals of 525 nm. At voltages lower than 50 V (10 V for SPL 2407), the APD gain can be regarded as unity since the photocurrent remained constant. Figure 1 (*left*) shows variations of APD gain as a function of bias voltage, measured at $+20^{\circ}\text{C}$. At a gain of 30, the gain variations on bias voltage are approximated by $+2.7\ \%/V$ for reverse-type APDs (S8664-55, S8664-1010N) whereas $+0.5\ \%/V$ for reach-through APD (SPL2407). Note that this is comparable to the voltage coefficient of typical PMTs ($\sim +2\ \%/V$).

As discussed in detail in Ikagawa et al.(2003) APD gain also depends on temperature. At a gain of 50, gain variations of APD ranges in a few $\%/^{\circ}\text{C}$, which is an order of magnitude larger than typical PMTs. Therefore, temperature control could be more critical problems for APDs. Throughout this paper, temperature was controlled in a thermostat within 0.1°C . Corresponding variations of gain is less than 0.3 %.

Figure 1 (*right*) shows the variations of capacitance as a function of bias voltage, measured at $+20^{\circ}\text{C}$. The capacitance of SPL 2407 is almost constant above the bias voltage of 150 V, whereas those of S8664-55 and S8664-1010 gradually decrease even above 300 V. The different behavior reflects the differences in the internal structure of these APDs: reach-through APD can be fully depleted at 150 V whereas $\geq 300\ \text{V}$ is required for reverse-type APDs.

2.3. Dark current

In Figure 2, the dark current of the APDs is plotted as a function of bias voltage for different temperatures (*left*; $+20^{\circ}\text{C}$ and *right*; -20°C). Note that dependences on bias voltage are quite similar to those of avalanche gains (Figure 1 *left*). This strongly suggests that most of the dark current is bulk dark current where all primary dark current carriers undergo the full gain of the APD: electrons are fully multiplied in the reach-through APD, whereas only hole multiplications occur in the reverse-type APD.

The leakage currents were measured at room temperature: 4.4 nA, 0.4 nA, and 1.7 nA at a gain of 30 for SPL 2407, S8664-55 and S864-1010N, respectively. There values are extremely low compared to those reported for the beveled-edge APDs of a similar size. For example Moszyński et al. (1998) reported that leakage current of 16 mm ϕ APD is $\geq 100\ \text{nA}$ at room temperature. For Hamamatsu APD, leakage current further decreases to 10–100 pA level at -20°C .

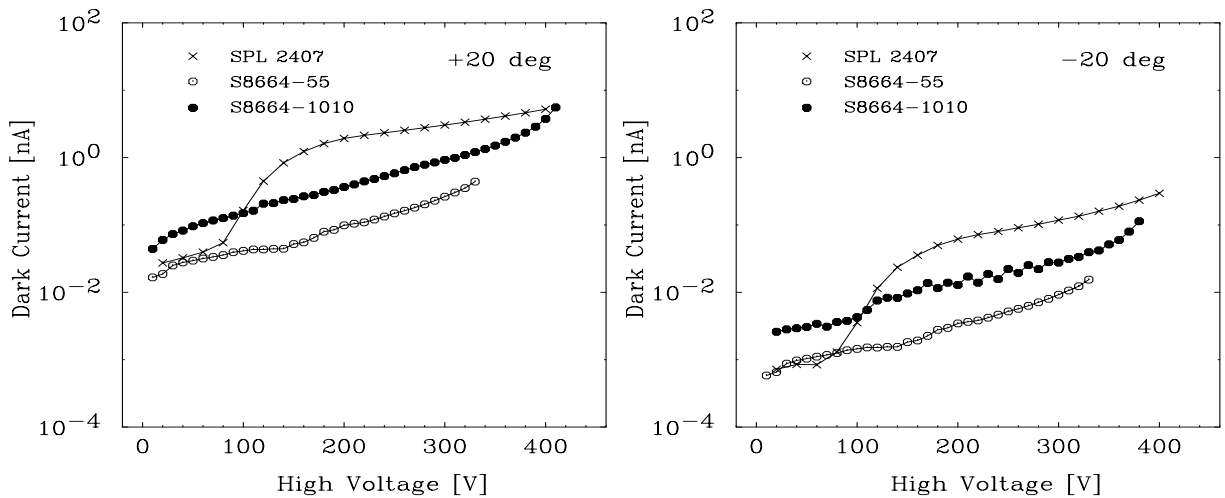


Figure 2. Dark current variations of Hamamatsu APDs measured at $+20^{\circ}\text{C}$ (*left*) and -20°C (*right*).

3. PERFORMANCE AS A SOFT X-RAY DETECTOR

3.1. Energy spectra

An incident X-rays interacts with the semi-conductor, and deposits its energy by creating electron-hole (e-h) pairs. In silicon, $h\nu/3.65$ eV pairs are produced where $h\nu$ is the X-ray energy and 3.65 eV is the work function for creating single pair of e-h. For example, number of electrons created in silicon by a 5.9 keV X-ray is ~ 1600 . This is about an order of magnitude larger than that created in gas counter, and hence possible energy resolution is extremely high. A silicon device of a $130\ \mu\text{m}$ thickness can potentially detect soft X-rays below 20 keV with efficiencies greater than 10% (Figure 3 *left*). In actual cases, however, electrical thermal noise in the detector and the pre-amplifier circuit limit the detectable lower threshold to ~ 10 keV when operating at room temperature. Therefore, semi-conductor devices for soft X-rays must be operated at liquid nitrogen temperatures to reduce the thermal noise.

As we have reviewed in §2.1, the signal amplification in the APD devices has a good advantage of detecting soft X-ras even at room temperature or at lightly cooled environment.²² Figure 3 (*right*) presents the energy spectrum of 5.9 keV X-rays from a ^{55}Fe source measured with SPL 2407 at -20°C . Note that energy threshold is as low as $E_{\text{th}} \sim 0.5$ keV. The K-shell peaks of Mn K_{α} and K_{β} are marginally resolved in the line profile. The FWHM width of the 5.9 keV peak was $\Delta E \sim 379$ eV (6.4 %; Figure 3 *right*), which is the best record ever achieved with APDs (see § 2.1). This resolution is clearly better than those obtained with the proportional counters, but still worse compared to the energy resolution of an X-ray CCD camera operated at heavily cooled environment ($\Delta E \sim 130$ eV at -60°C ¹⁰).

3.2. High-rate counting

Fast timing is another excellent property of APDs. It has been reported that an APD with a few mm^2 detection area has fast timing properties better or comparable to that of a fast PMT. Kishimoto et al. (1998; 2001) have developed a fast counting system utilizing stacked APDs (SPL 2625; reach-through type) for X-ray diffraction experiments with synchrotron radiation. They showed that pulse height measurements at output rates of up to 10^8 cts/s were successfully carried out by sequential single-channel discrimination.

Motivated by their experiments, we have tested the counting response of SPL 2407 using a monochromatic X-ray beam at a beamline BL-14A of the Photon Factory (KEK-PF) in Tsukuba, Japan. Fast amplifiers (Phillips 6954; gain = 100) are used for amplifying the signal from APD. The signals from the amplifier was sent to a NIM discriminator (Phillips 704) and outputs were recorded by a visual scaler. Figure 4 (*left*) shows an observed amplifier outputs for a 5.9 keV X-ray. This clearly demonstrates that signal carriers in the APD device are

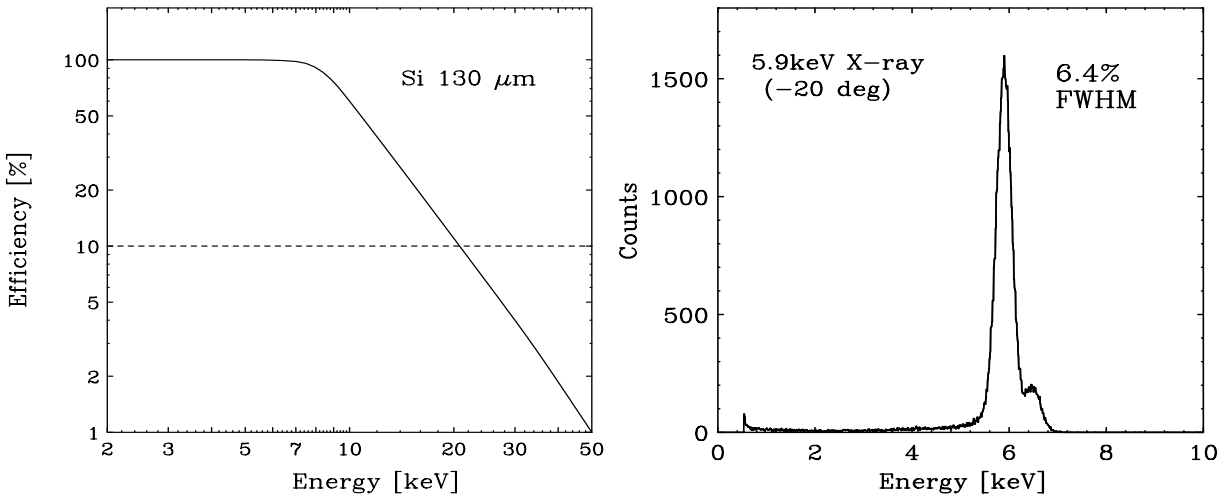


Figure 3. *left:* Detection efficiency of SPL 2407 (130 μm of Si) in direct detection of X-rays. *right:* Energy spectrum of 5.9 keV X-rays measured at -20°C .

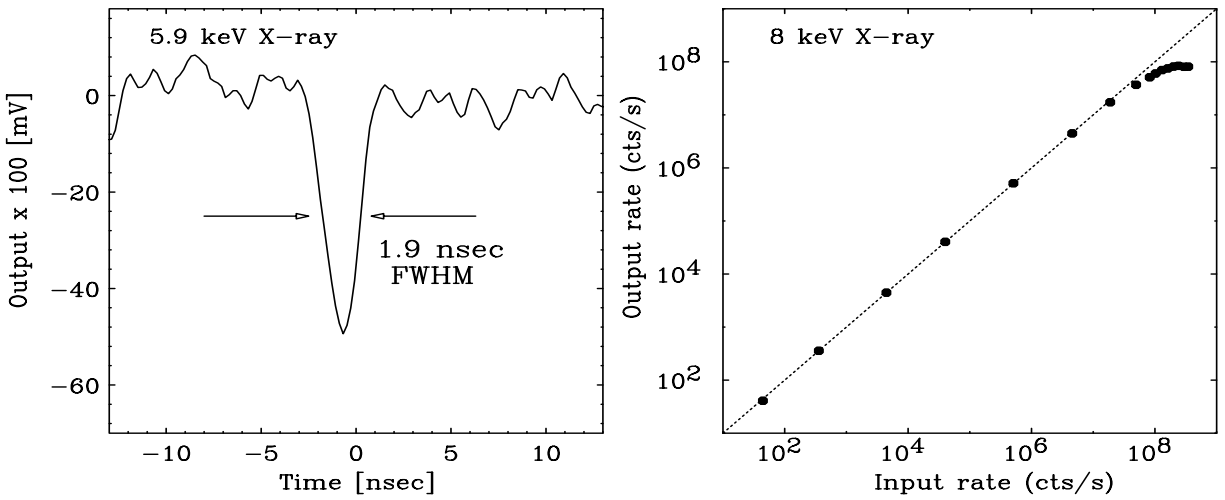


Figure 4. *left:* An observed signal of current amplifier output of a 5.9 keV X-ray. *right:* Output count rate as a function of the input (observed) photon rate for 8.0 keV X-rays.

collected within a short time interval of 1.9 nsec (FWHM). Also note that noise fluctuation is as low as 1 keV (~ 8 mV compared to 48 mV for 5.9 keV signal) even with this simple data acquisition system.

Figure 4 (*right*) presents the output count rate as a function of the input (observed) photon rate for 8.0 keV photons. More than 34 % signals was successfully recorded at the maximum input rate of $\sim 8 \times 10^7$ cts/s. Since the noise level of the APD detector is less than 10^{-2} cts/s, we obtain a dynamic range of more than 10^9 . Since this type of APD (reach-through type) can also work as a charged particle detector, we plan to use it as a high-counting particle monitor onboard the forthcoming Pico-satellite Cute1.7.⁷ This will be the first mission of using APDs in space as a scientific instrument, and study the distribution of low-energy ($E \leq 30$ keV) electrons and protons trapped in the South Atlantic Anomaly (SAA) and aurora band.

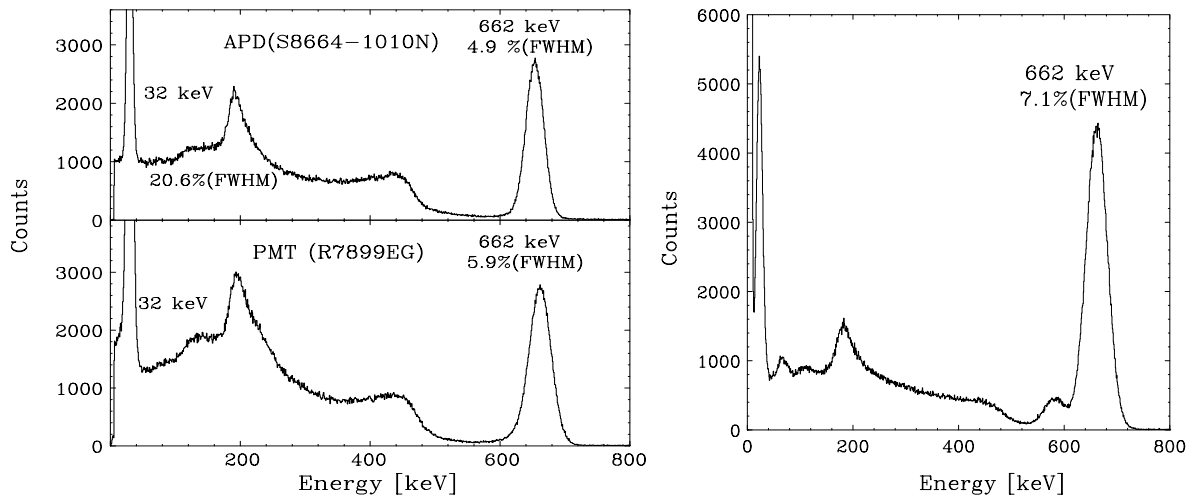


Figure 5. *left:* Energy spectrum of ^{137}Cs obtained with CsI(Tl) crystal coupled to a large area APD (S8664-1010N: *top*) and PMT (R7899EG: *bottom*), measured at $+20^\circ\text{C}$. *right:* Energy spectrum of ^{137}Cs obtained with BGO crystal coupled to a large area APD (S8664-1010N), measured at -20°C .

4. PERFORMANCE AS A SCINTILLATION PHOTON DETECTOR

4.1. Read-out of various scintillators

In this section, we study the performance of reverse-type APD, S8664-1010N, as a γ -ray detector coupled with four different scintillators; CsI(Tl), BGO, GSO(Ce) and YAP(Ce). A size of the crystals was $10\times 10\times 10\text{ mm}^3$, and can fully match the sensitive area of the APD. The crystals were wrapped with several layers of Teflon tape, and were coupled with silicon rubber sheet ($100\ \mu\text{m}$ thickness) directly to the entrance window of S8664-1010N. We also measured the pulse height spectra with the PMT for comparison (Hamamatsu R7899EG; 1 inch diameter), using the same scintillation crystals.

Since the QE of reverse-type APD peaks at visible and near infrared, $500\text{--}830\text{ nm}$, CsI(Tl) crystal (peak emission at 550 nm) is well matching to be used with APDs. Figure 5 (*left*) compares the pulse height spectra for 662 keV γ -rays from a ^{137}Cs source, measured with a CsI(Tl) crystal at room temperature ($+20^\circ\text{C}$). Thanks to a high QE of more than 80%, an excellent FWHM energy resolution of $4.9\pm 0.2\%$ was obtained for the APD (*upper*), which is much better than that obtained with the PMT (*lower*: $5.9\pm 0.1\%$ FWHM). More strikingly, APDs' internal gain reduces electric noise contribution significantly. As we can see in Figure 5, both the APD and the PMT could resolve K-shell X-ray peak at 32 keV . Such a low energy peak could not be resolved when the CsI(Tl) crystal was coupled with photo diodes. The energy resolutions of 32 keV X-rays were $20.6\pm 0.2\%$ for the APD, and $23.0\pm 0.1\%$ for the PMT.³

Table 2. Comparison of FWHM energy resolutions for 662 keV γ -rays, measured at $+20^\circ\text{C}$.

| Crystal | APD ($+20^\circ\text{C}$) | APD (-20°C) | PMT($+20^\circ\text{C}$) |
|---------|-----------------------------|-----------------------------|----------------------------|
| CsI(Tl) | $4.9\pm 0.2\%$ | $5.9\pm 0.1\%$ | $5.9\pm 0.1\%$ |
| BGO | $8.3\pm 0.2\%$ | $7.1\pm 0.2\%$ | $10.4\pm 0.1\%$ |
| GSO(Ce) | $7.8\pm 0.2\%$ | $7.1\pm 0.2\%$ | $9.3\pm 0.1\%$ |
| YAP(Ce) | $11.3\pm 0.3\%$ | $10.7\pm 0.2\%$ | $12.4\pm 0.1\%$ |

Similarly, the large are APD is superior to the PMT when coupled with various scintillators (BGO, GSO(Ce), YAP(Ce)) as listed in Table 2. These scintillators have peak emissions at relatively short wavelengths ($350\text{--}480$

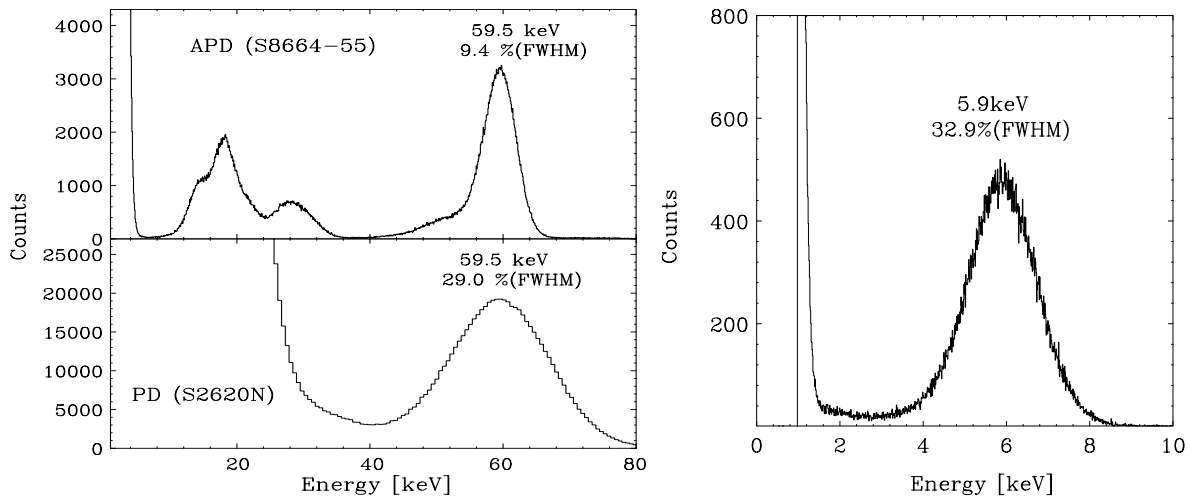


Figure 6. *left:* Energy spectra of 59.5 keV γ -rays from a ^{241}Am source measured with a CsI(Tl) crystal coupled to the APD (S8664-55: *upper*) and the PD (S2620N). *right:* ^{55}Fe spectrum measured at -20°C with CsI(Tl) crystal.

nm), where the APD is less sensitive (QE $\sim 60\%$ at 390 nm) compared to the CsI(Tl) crystal. Nevertheless, QE of the APD is still much larger than that of the PMT (QE $\sim 20\%$), resulting in better energy resolutions. Figure 5 (*right*) shows the energy spectrum of 662 keV γ -rays at -20°C , measured with S8664-1010N coupled to a BGO crystal. A good energy resolution of $7.1 \pm 0.2\%$ was obtained for 662 keV γ -rays. The minimum detectable energy was 11.3 keV.

Finally, we compare the 662 keV full energy peak detected in the scintillator to that of 5.9 keV X-rays from a ^{55}Fe source detected directly by the APD. This provides a good reference to measure number of e-h pairs created in the APD device. We found that 6100 ± 400 e-h pairs are created in the APD per 1 MeV at -20°C .³ This result is consistent with a light collection of BGO scintillator, and corresponds to 60–70 % of scintillation light yield reported by manufacture (8000–10000 photon/MeV).

4.2. Low energy scintillation detection

Low leakage current of the reverse-type APD should have an excellent advantage for the detection of a low level of scintillation light, corresponding to γ -ray energy below 100 keV. In the case of beveled-edge APDs, the best FWHM resolutions of $11.3 \pm 0.3\%$ and $8.4 \pm 0.3\%$ have been reported so far for 59.5 keV γ -rays and 122 keV γ -rays respectively, as measured with a 10 mm diameter \times 10 mm high NaI(Tl) crystal.¹² These are clearly nice results, however, we should remind that the device dark noise still significantly affects the energy resolution below 50 keV. Hamamatsu reverse-type APDs have much lower leakage current ($\sim 1/100$ of beveled-edge APDs; §2.3) that should improve their results further. To demonstrate the advantage of reverse-type APDs, we measured a CsI(Tl) crystal ($5 \times 5 \times 5 \text{ mm}^3$) which can fully match the sensitive area of the S8664-55.

Figure 6 (*left*) shows the pulse height spectrum of 59.6 keV γ -rays from an ^{241}Am source, measured at room temperature ($+20^\circ\text{C}$; figures from Ikagawa et al. 2003). The pulse height spectra, using the same CsI(Tl) scintillator coupled to the PIN-photodiode (Hamamatsu S2620N-1771: $5 \times 5 \text{ mm}^2$ surface) is also shown for comparison. Significant difference can be seen in the low-energy part of the spectra. A combination of 14–21 keV lines of Np (L_α , L_β and L_γ) is clearly resolved for APD whereas noise dominates for PIN-PD. Energy resolutions of 59.6 keV γ -rays are $9.4 \pm 0.3\%$ for the APD and $29.0 \pm 0.2\%$ for the PIN-PD, respectively. The energy resolutions we have achieved with APD for low energy γ -rays, are one of the best records ever reported for scintillation detectors.

As reported in literature,² minimum detectable energy of CsI(Tl) scintillation light is as low as 4.6 keV at room temperature ($+20^\circ\text{C}$), and improves significantly as decreasing temperature. At -20°C , E_{th} reaches to 1.1 keV. Figure 6 (*right*) shows the ^{55}Fe spectra measured at -20°C , with S8664-55. A 5.9 keV peak is

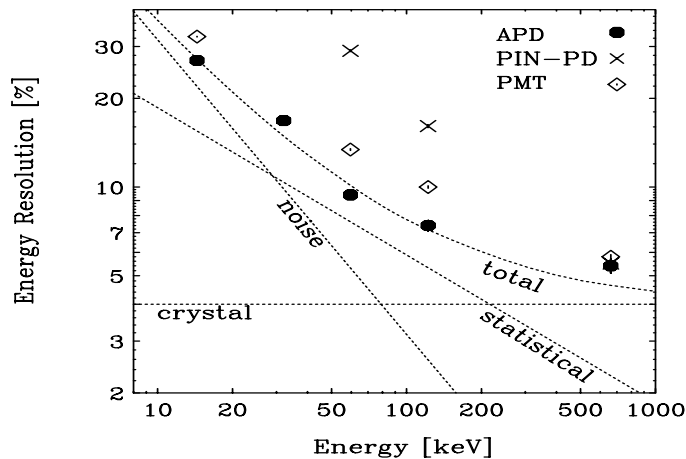


Figure 7. Energy resolution of CsI(Tl) crystal versus energy of γ -rays. The dotted lines represent the contribution of electric noise, statistical noise, and intrinsic resolution of scintillator.

clearly resolved with the energy resolution of 32.9 ± 0.3 % (FWHM). Note that, the energy resolution is better or comparable to those obtained with cleaved NaI(Tl) crystal coupled to PMT (typically 35–50 % for 5.9 keV X-rays).

Figure 7 summarizes the energy resolutions of CsI(Tl) crystal plotted versus energy of γ -rays in the range of 14.4 keV to 662 keV, measured at room temperature ($+20^\circ\text{C}$). The dotted lines represent the contribution of dark noise of the APD, statistical fluctuation, and the intrinsic resolution of the crystal. Thanks to the internal gain and high QE, the energy resolutions of CsI(Tl) crystal measured with APD are much better than those obtained with the PMT and the photo diode below 1 MeV.

5. APPLICATIONS

5.1. Application to the Japanese X-ray astronomy mission *NeXT*

Large-area APDs can effectively collect weak scintillation light from large size crystals. As an application, we tried to read out large BGO plate ($300 \times 48 \text{mm}^2$ surface and 3mm thickness) with the $10 \times 10 \text{mm}^2$ APD (S8664-1010N). Light signals from a cross section of the BGO crystal were transmitted to the APD through a light-guide. Figure 8 (*left*) presents an energy spectrum of ^{137}Cs measured at -15°C . Despite significant mismatch of the scintillator size and APD surface area, this APD was able to collect a large number of scintillation photons. A good energy resolution of 20.9 ± 0.2 % was obtained for 662 keV γ -rays with the minimum detectable energy (E_{th}) of about 60 keV.³

This result suggests various possibilities of using APDs for future applications. For example, we have a plan to use APDs for Japan’s future X-ray astronomy mission *NeXT* (New X-ray Telescope), which is planned to be launched in ~ 2011 .²⁰ The *NeXT* mission is a successor to the Astro-E2 mission (planned to be launched in 2005), with much higher sensitivity in the energy from 0.5 keV to 1 MeV. In the energy range above ~ 100 keV, shielding against background becomes important because signals from celestial sources are much weaker than the background events, some from diffuse cosmic γ -rays and others may have atmospheric origin. Moreover, geomagnetically trapped particles and primary cosmic rays are serious matters to cope with. The phoswich configuration and a tight and active “well-type” shield is a good solution to reduce the background significantly.

We have proposed a new detector called the Soft Gamma-ray Detector (SGD) for the *NeXT* mission, which utilizes the idea of a narrow FOV Compton telescope as shown in Figure 8. In the SGD, we combine a stack of Si strip detectors and CdTe pixel detectors as a detection part, which is mounted inside the well-type BGO active shield. We are planning to use APDs to read out Well and Bottom BGO scintillators, instead of PMTs.

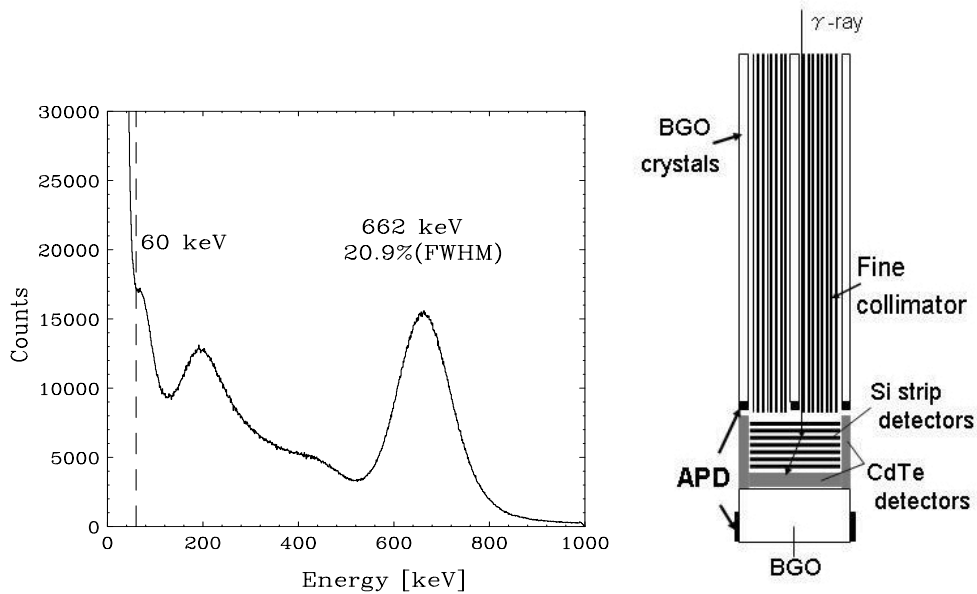


Figure 8. *left:* Energy spectrum of ^{137}Cs measured with S8664-1010N coupled to a large BGO plate ($300\times 48\text{ mm}^2$, 3mm thickness) at -15°C . *right:* The configuration of a unit of soft γ -ray detector onboard the *NeXT* satellite.

Dimensions of Well BGO plate will be similar to that measured in this section. Since the APD is very compact and have ragged structure, we can directly couple APD with BGO plate to read out weak scintillation photons.

We have shown that the minimum detectable energy could be as low as 60 keV for the APD plus BGO plate system, but we expect that E_{th} can be further improved as (1) APD size is still far from optimum, and (2) significant fraction of scintillation light may be lost when transmitting the light guide. We will develop new types of large area APD (e.g., $50\times 3\text{ mm}^2$ rectangular size) which can fully match the surface edge of the Well BGO plate, and hope to realize E_{th} of $\sim 30\text{ keV}$.

5.2. 4ch Anger camera

Anger-type γ -ray camera is invented by H. Anger in the 1950s.¹ The principle idea is at the basis of almost all cameras used in current day nuclear imaging. It consists of a collimator, the detector, and an 2-dimensional array of light sensors. In the original configuration, the detector is a single crystal of NaI(Tl), and scintillation light were detected by PMT arrays which are optically coupled to the surface of the crystal. Depending on the position of input γ -rays, the output signals from the PMT varies, such that the PMT closest to the incident position output the largest signal, whereas farthest PMT output the smallest signal.

If the PMTs are replaced by APDs, the imaging system can be compact and more flexibly used in various applications. Figure 9 (*left*) shows the concept of ‘‘APD Anger camera’’ tested in this paper. A large CsI(Tl) crystal, $50\times 50\text{ mm}^2$ and 10 mm thickness, was used as a γ -ray detector. Output signals from 4 APDs, which were placed just behind the corner of the CsI(Tl) crystal, are recorded by computer. We calculate the ‘‘weighted mean’’ of four APD outputs, and converted it to the X-Y position on the detector plane. We measured the response of APD camera using a monochromatic X-ray beam (70 keV) at beamline BL-14A of the Photon Factory (KEK-PF) in Tsukuba, Japan. The CsI(Tl) was scanned with the collimated 70 keV beam ($0.1\times 0.1\text{ mm}^2$) at 10 mm intervals, in both X and Y-axis direction. We obtained 25 points data in total.

Figure 9 (*right*) shows example images corresponding to five different positions; four corners and one center of the CsI(Tl) crystal. The best positional resolution of 5mm (FWHM) were obtained at the corners, whereas the resolution significantly degraded at the center (15 mm FWHM). Apparently, this is due to the fact that we did not place APD sensor just behind the center of the CsI(Tl) crystal. In such a situation, incident position of

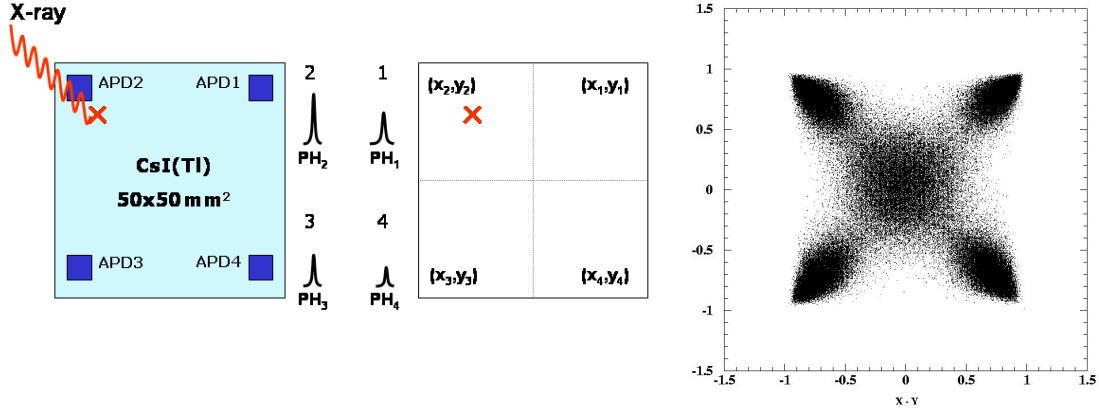


Figure 9. *left:* The schematic diagram of 4ch Anger camera developed in this paper. *right:* A superposed image of collimated X-ray beam (70 keV) injected at five different positions; four corners and one in the center.

γ -rays is quite uncertain since the scintillation light must be equally shared by the corner APDs. Nevertheless, 15 mm resolution is much better than an interval of APDs placed behind the crystal (≥ 40 mm).

5.3. 32ch APD array

In the previous section, we have reviewed the basic principle of an Anger camera, but of course, it is oversimplified in many aspects. For more realistic applications, “APD arrays” have been successfully fabricated by different manufactures. Pixel arrays offer new design options for physics experiments and nuclear medicine, such as imaging devices for positron emission tomography (PET). Hamamatsu S8550 (reverse-type; Figure 10 *left*) is a monolithic 8×4 pixels structure with a surface area of 2×2 mm² for each pixel. The common cathode and the individual anode of the 32 diodes are connected at the backside of the carrier plates. We are testing the performance of S8550, and are developing read-out electronics for imaging purposes. Initial results are also found in literature.⁴

The leakage current of S8550 is quite uniform between 16 pixels: 1.4–1.9 nA at a gain of 50, measured at $\lambda = 420$ nm. Capacitance of each pixel ranges in 9–11 pF. APD signals were read out from the anode of the APD, cutting the DC component by the coupling condenser of 2.2 nF. The signals of the APD were amplified by 32ch charge sensitive amplifier (CSA 5027; Figure 10 *right*) and fed to the shaping amplifier (CP 4066), both provided by Clearpulse Co. Charge conversion factor of CSA is 2V/pC, and noise equivalent charge is 329–493 electrons at 0pF (for Si) The pulse height of the shaping amplifier was digitized by the 12 bit VME analog to digital converter (Clearpulse 1113), and recored by computer.

Figure 11 presents energy spectra obtained for 32 pixels of S8550 using 5.9 keV X-rays. The pixel-to-pixel gain non-uniformity was measured to be less than $\pm 3\%$ at a gain of 50. Kapsta et al. (2003) also measured crosstalk by illuminating the center of a pixel with a light spot and recording the amplitude spectra from the neighboring pixels protected against the light. They reported that highest crosstalk between adjacent pixels was 4% at a device gain of 60. These reports promise the applicability of Hamamatsu APD array in nuclear medicine and experimental physics near future. We are stating to develop a γ -ray imaging detector based on the APD arrays coupled to CsI(Tl) crystals, and results will be discussed in detail in Saito et al. (2004).

6. CONCLUSION

We have studied the performance of large area APDs recently developed by Hamamatsu Photonics K.K. After reviewing the APD structures and basic parameters of each APDs, we show that reach-through APD can be

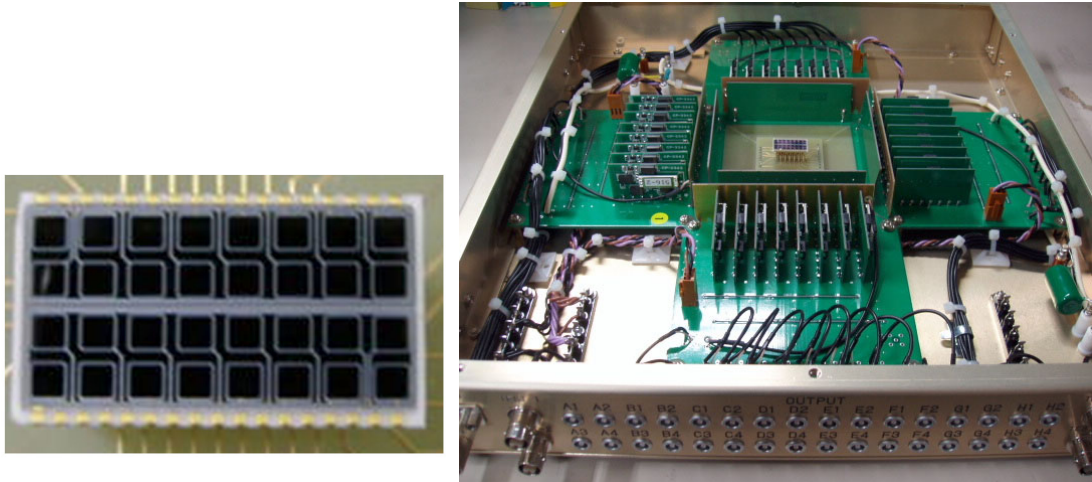


Figure 10. *left:* A unit of 32 ch APD array tested in this paper. *right:* Charge sensitive amplifier, CSA 5027, specifically designed to readout signals from APD pixel arrays.

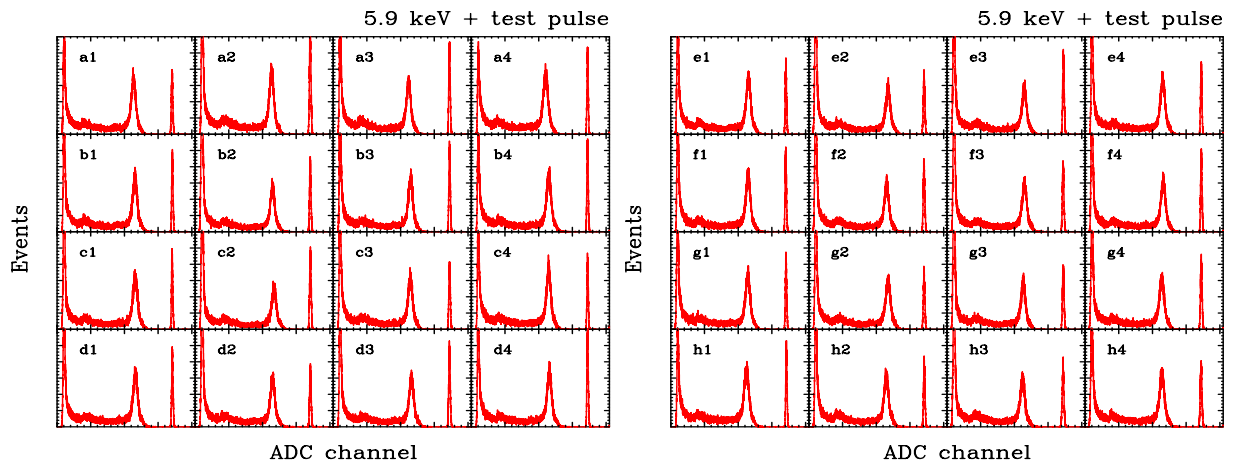


Figure 11. A matrix of ^{55}Fe spectra taken with each individual pixels of APD detector array.

an excellent soft X-ray detector operating at room temperature or moderately cooled environment. We obtain the best energy resolution ever achieved with APDs, 6.4 % for 5.9 keV X-rays, and obtain the energy threshold as low as 0.5 keV measured at -20 °C. As a scintillation photon detector, reverse-type APDs have an great advantage of reducing the dark noise significantly. We obtain the best FWHM energy resolutions of $4.9\pm 0.2\%$ and $9.4\pm 0.3\%$ for 662 keV and 59.5 keV γ -rays, as measured with a CsI(Tl) crystal. Moreover, 5.9 keV X-rays are clearly resolved with an FWHM resolution of $32.9\pm 0.3\%$. Combination of APDs with various other scintillators (BGO, GSO, and YAP) also showed better results than those obtained with the PMT. These results suggest that APD could be a promising device for replacing traditional PMT usage in some applications. For example, we are planning to use APDs for Japan's future X-ray astronomy mission *NeXT*. Also, compact APD camera and pixel arrays offer new design options for physics experiments and nuclear medicine near future.

ACKNOWLEDGMENTS

We would like to thank Dr. S. Kishimoto for useful comments and discussion about the APD device in general.

REFERENCES

1. H.O. Anger, Rev. Sci. Instr. 29 (1958) 27
2. T. Ikagawa, J. Kataoka, Y. Yatsu et al. Nucl. Instr. and Meth, A, 515 (2003) 671
3. T. Ikagawa, J. Kataoka, Y. Yatsu et al. Nucl. Instr. and Meth, (2004), submitted
4. M. Kapusta, P. Crespo, D. Wolski, M. Moszyński, and W. Enghardt, Nucl. Instr. and Meth, A, 504 (2003) 139
5. S. Kishimoto, N. Ichizawa, & T.P. Vaalsta, Rev. of Sci. Inst, 69, 2 (1998) 384
6. S. Kishimoto, H. Adachi, & M. Ito, Nucl. Instr. and Meth, A, 467–468 (2001) 1171
7. Y. Kuramoto, et al. in preparation
8. R. Lecomte, C. Pepin, D. Rouleau, H. Dautet, R. J. McIntyre, D. McSween, and P. Webb, Nucl. Instr. and Meth, A, 423 (1999) 92
9. R.J. McIntyre, P.P. Webb, H.Dautet, IEEE Trans. Nucl. Sci., 43 (1996) 1341
10. E.Miyata et al., SPIE, Vol. 5165 (2003) 366
11. M. Moszyński, M. Kapusta, D. Wolski, M. Szawlowski, and W. Klamra, IEEE Trans. Nucl. Sci., 45 (1998) 472
12. M. Moszyński, M., M. Kapusta, J. Zalipska, M. Balcerzyk, D. Wolski, M. Szawlowski, and W. Klamra, IEEE Trans. Nucl. Sci., 46 (1999) 880
13. M. Moszyński, M. Kapusta, M. Balcerzyk, M. Szawlowski, D. Wolski, I. Wegrecka, and M. Wegrzecki, IEEE Trans. Nucl. Sci., 48 (2001) 1205
14. M. Moszyński, W. Czarnacki, M. Szawlowski, B.L. Zhou, M. Kapusta, D. Wolski, and P. Schotanus, IEEE Trans. Nucl. Sci., 49 (2002a) 971
15. M. Moszyński, M. Szawlowski, M. Kapusta, M. Balcerzyk, Nucl. Instr. and Meth, A, 485 (2002b) 504
16. M. Moszyński, M. Szawlowski, M. Kapusta, M. Balcerzyk, Nucl. Instr. and Meth, A, 497 (2003) 226
17. A. Ochi, Y. Nishi, and T. Tanimori, Nucl. Instr. and Meth, A, 378 (1996) 267
18. T. Saito, et al. in preparation
19. V. Solovov, F. Neves, V. Chepel, M. I. Lopes, R.F. Marques, and A.J.P.L. Policarpo, proceeding of “3rd International Conference on New Developments on Photodetection”, Beaune, France, (2002), June 17-21
20. T. Takahashi et al., New Astronomy Reviews, 48 (2004) 269
21. P.P. Webb, R.J. McIntyre, and J. Cornadi, RCA Review, 35 (1974) 234
22. Y. Yatsu, J. Kataoka, Y. Kuramoto et al. Nucl. Instr. and Meth, (2004), submitted